

Global Distribution of Spatial Correlation Coefficient of Rainfall Rate
Inferred from Measurement of Spaceborne Radar

Yuji OHSAKI
Communications Research Laboratory
4-2-1 Nukuikita-machi, Koganei-shi, Tokyo 184-8975, Japan

1 Introduction

Precipitation is a serious source of attenuation for microwave communication links, and the performance of microwave communication system is strongly influenced by the quantity and characteristic of precipitation. Taking the spatial inhomogeneity of rainfall rate into consideration, Morita and Higuti [1] proposed a method (M-H method) for predicting rain attenuation. In this method the spatial structure of rain is statistically represented by the spatial correlation coefficient α of the rainfall rate.

Since the spatial structure of rain is affected by regional differences in climate and rain type [2], the value of α has dependence on regional differences. Morita and Higuti determined α by using a rain gauge network in Tokyo, Japan [3]. This type of evaluation is quite laborious and has been done for few localities. Furthermore, the spatial correlation coefficient measured in Japan does not always hold throughout the world due to the dependence on regional differences. Thus, when the M-H method is used for predicting rain attenuation, the value of α determined in the relevant area should be used. The Tropical Rainfall Measuring Mission (TRMM) is a spaceborne radar project of the United States and Japan [4]. The first spaceborne rain radar is aboard the TRMM satellite. The TRMM can provide quantitative measurements of rainfall over all land and ocean areas of the tropics. Global distribution of α has been inferred from TRMM measurement.

2 Global distribution of α

The spatial correlation function $\rho(d)$ of the rainfall rate R (mm/h) expresses the correlation coefficient of R 's separated by a distance d (km). Two types of formula for $\rho(d)$ have been proposed (F_1 and F_2), which are given by:

$$F_1 : \rho(d) = \exp(-\alpha_1 d), \quad (1)$$

and

$$F_2 : \rho(d) = \exp(-\alpha_2 \sqrt{d}), \quad (2)$$

where α_1 (km^{-1}) and α_2 ($\text{km}^{-\frac{1}{2}}$) are parameters called the spatial correlation coefficient of R . Manabe et al. showed that $\rho(d)$ given by Eq. (1) was appropriate for Europe [5], and Morita and Higuti showed that $\rho(d)$ given by Eq. (2) was appropriate for Japan [3]. These two types of $\rho(d)$ formulas are used to estimate global distribution of α .

The standard TRMM data products are categorized into three levels (1, 2, and 3). Level 1, 2, and 3 products mainly handle engineering values, physical values, and statistical values, respectively. All product levels are created by the National Space Development Agency of Japan and the National Aeronautics and Space Administration. The TRMM 2A25 is level 2 product. The TRMM 2A25 data used in this study was measured in May and June 1998, and June and July 1999. TRMM can measure the rain at latitude ± 37 degrees. Global distribution of α is estimated at longitude from 0 to 360 degrees, and at latitude ± 36 degrees with grid size of 2.0 by 2.0 degrees. Smaller grid size is better for estimating global distribution of α with fine spatial resolution. However, as grid size becomes smaller, the amount of data in each grid becomes smaller. A sufficient amount of data should be used to determine α , and a grid size of 2.0 by 2.0 degrees was determined for this reason. The amount of data for each grid ranges from about 2.0×10^4 to 1.2×10^5 .

To achieve a 200-km swath, the TRMM radar scans between 17.0 and -17.0 degrees from the nadir using 49 angle bins. Figure 1 shows a conceptual illustration of this scan. R_i is the rainfall rate (mm/h) for each range bin. The integer index i is from $i = 1$ to $i = n$. R_1 is located at near ground, and R_n is located at the storm height [6]. Distance between each range bin is 0.25 km. $\rho(d)$ is calculated from the following equation.

$$\rho(0.25 \times (i - 1)) = \sqrt{\frac{\text{Cov}(R_1, R_i)}{\text{Var}(R_1) \times \text{Var}(R_i)}}, \quad (3)$$

where $\text{Cov}(R_1, R_i)$ is covariance between R_1 and R_i , $\text{Var}(R_1)$ is variance of R_1 , and $\text{Var}(R_i)$ is variance of R_i . $\rho(d)$ is calculated at longitude from 0 to 360 degrees, and at latitude ± 36 degrees with grid size of 2.0 by 2.0 degrees. If R_1 is located in a grid, angle bin data including this R_1 is used for calculating $\rho(d)$ in this grid.

Rain/no-rain discrimination for TRMM is done for each angle bin [6]. Rain discriminated angle bins are used only for calculation of $\rho(d)$. Figure 2 shows global distribution of percentage of rain data (P) in terms of the total amount of data for each grid. P is less than 10% in many grids. Morita and Higuti used 10% of the conditional time to accurately express the rainfall rate distribution by a lognormal distribution [1]. The value of 10% of the conditional time is also used to estimate $\rho(d)$ by measurement with a rain gauge network. If the percentage of the time during which it rains, (P_t), is less than 10% of the total measurement time, then 10% of the conditional time, which includes rain and no-rain periods, can be used to accurately express the rainfall rate distribution by a lognormal distribution.

We also use the value of 10% of the conditional time to estimate $\rho(d)$ by TRMM measurements. While a rain gauge can continuously measure rain in time at a fixed point. TRMM can continuously measure rain in space. But its measurement is temporally discrete at a fixed point. We guess that if TRMM measurements at a fixed point had taken frequently, P would have been equal to P_t . When P is less than 10% for each grid,

10% of the conditional time has been applied to estimation of $\rho(d)$.

Figure 3 shows an example of calculated $\rho(d)$ indicated by black dots. The grid of this example is located at 139.0 degrees longitude and 35.0 degrees latitude, and includes Tokyo, Japan. The maximum range of the black dots corresponds to the mean value of storm height + its standard deviation. The mean value of storm height and its standard deviation in this grid are about 6.0 km and 1.0 km, respectively. The black dots are fitted by Eqs. (1) and (2) using least-squares fit. In this fitting, $\alpha_1 = 0.24$ and $\alpha_2 = 0.34$. Morita and Higuti assumed that $\alpha_2 = 0.35$ for a satellite-to-earth link [1]. $\alpha_2 = 0.35$ is fairly close to our result. As shown in Fig. 3, the black dots are fitted well by Eq. (2), and they are not fitted well by Eq. (1). Morita and Higuti showed that $\rho(d)$ given by Eq. (2) was appropriate for Japan [3]. Our results support those of Morita and Higuti's research.

Figures 4 and 5 show global distribution of α_1 and α_2 , respectively. In the least-squares fit calculation, the accuracy of parameters (e) is estimated. White gaps in these figures correspond to grids having large error of estimated parameter (larger than 100% of relative error). Relative error is calculated from $\frac{e}{\alpha} \times 100\%$. Grids having large error correspond well to those having small P as shown in Fig. 2. This suggests that α can not be correctly estimated from a small amount of rain data.

3 Discussion and concluding remarks

Figures 6 and 7 show global distribution of relative error of α_1 and α_2 , respectively. White gaps in these figures correspond to grids having large error of estimated α_1 and α_2 (larger than 100% of relative error). If $\rho(d)$ has dependence on regional differences, relative error of α_1 is always smaller than that of α_2 , or relative error of α_2 is always smaller than that of α_1 at a certain region. However, no clear dependence on regional differences can be found in Figs. 6 and 7.

Dependence of α on angle bin was investigated by calculating α for each angle bin. However, no clear dependence of α on angle bin was found. Miyagawa investigated dependence of α on elevation angle [7]. This investigation showed that when elevation angle becomes high, α becomes almost constant. The results of Miyagawa's study support those of this study.

This kind of study should use a large amount of data collected over a long term. However, the period of the present study was only four months. It is a fairly short term for a statistical study. The aim of this study is to investigate how to estimate α using TRMM data before attempting analysis using a large amount of data.

References

- [1] K. Morita and I. Higuti, "Statistical studies on rain attenuation and site diversity effect on earth to satellite links in microwave and millimeter wavebands," Trans. IECE, vol.E61, 6, pp.425-432, 1978.

- [2] D. M. A. Jones and W. M. Wendland, "Some statistics of instantaneous precipitation," J. Climate Appl. Meteor., vol.23, pp.1273-1285, 1984.
- [3] K. Morita and I. Higuti, "Prediction method for rain attenuation distribution of micro and millimeter waves," Rev. Electr. Commun. Labs., vol.24, pp.651-668, 1976.
- [4] J. Simpson, R.F. Adler, and G.R. North, "A proposed Tropical Rainfall Measuring Mission (TRMM) satellite," Bull. Amer. Meteor., vol.69, pp.278-295, 1988.
- [5] T. Manabe, H. Kobayashi, T. Ihara, and Y. Furuhashi, "Spatial correlation coefficients of rainfall rate intensity inferred from statistics of rainfall intensity and rain attenuation," ANN. Telecommun., vol.41, pp.463-469, 1986.
- [6] Y. Ohsaki, K. Nakamura, and T. Takeda, "Simulation-based analysis of dependence of the mean storm height measured by a spaceborne radar on its angle from the nadir," J. Atmos. Oceanic Technol., vol.18, pp.1127-1135, 2001.
- [7] Y. Miyagawa, "Dependence of spatial correlation function of rainfall rate on elevation angle," Review of the Radio Research Labs., vol.34, pp.13-22, 1988.

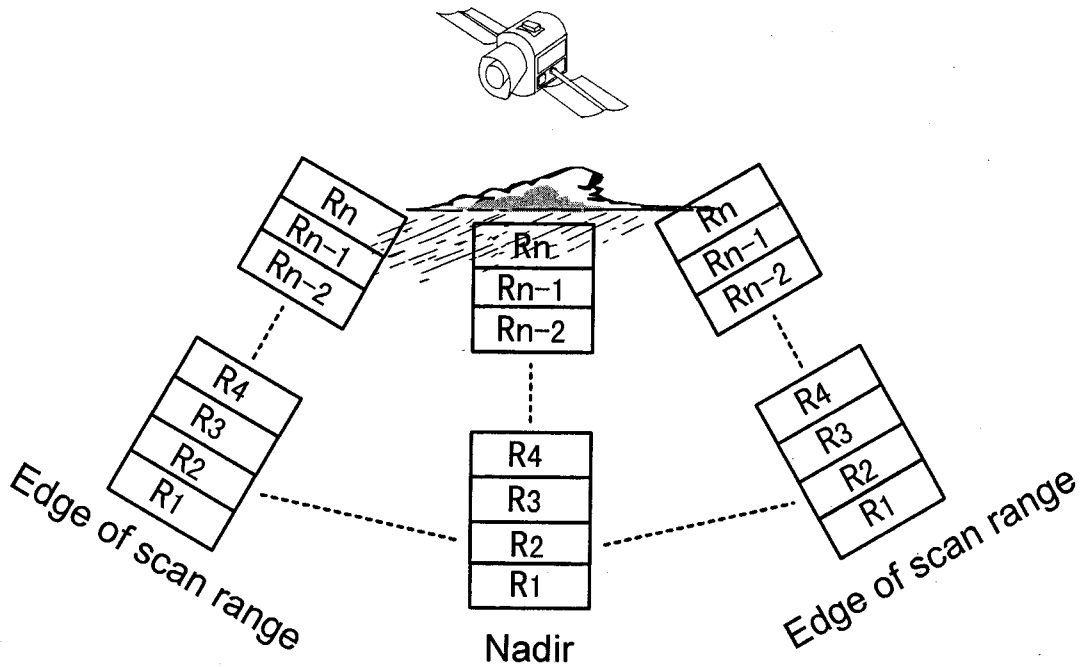


Fig. 1. Conceptual illustration of antenna scanning.

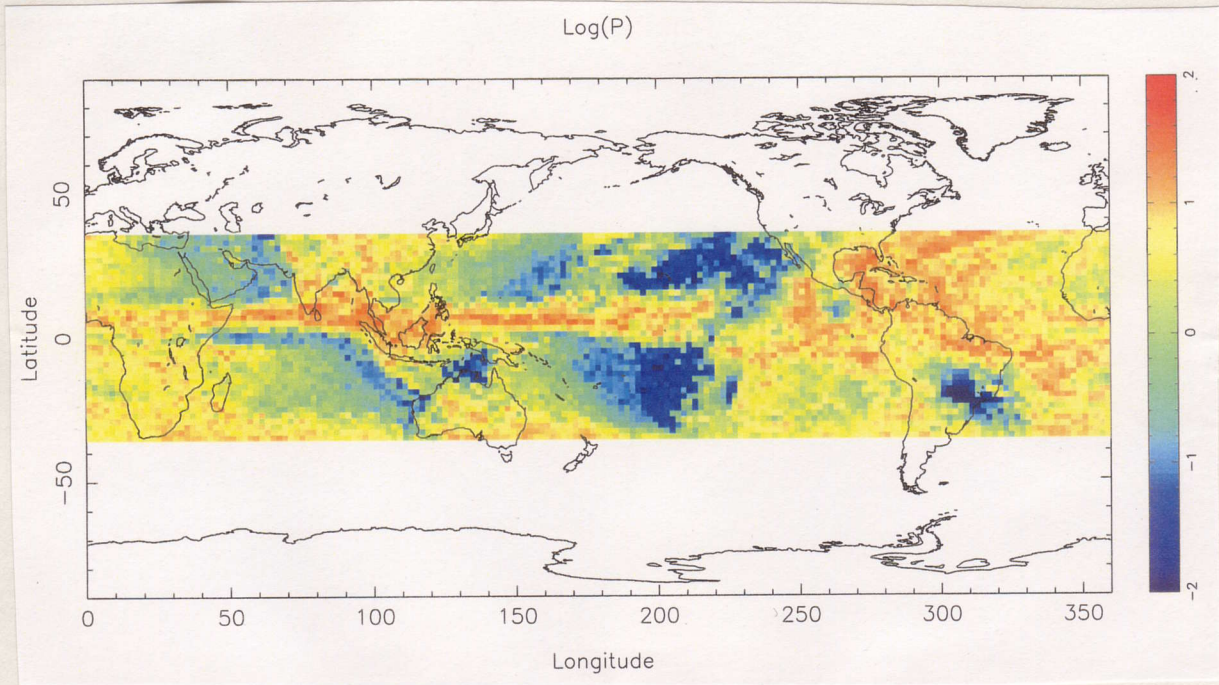


Fig. 2. Global distribution of percentage of rain data (P) in terms of total amount of data for each grid. Color bar values indicate logarithms of P .

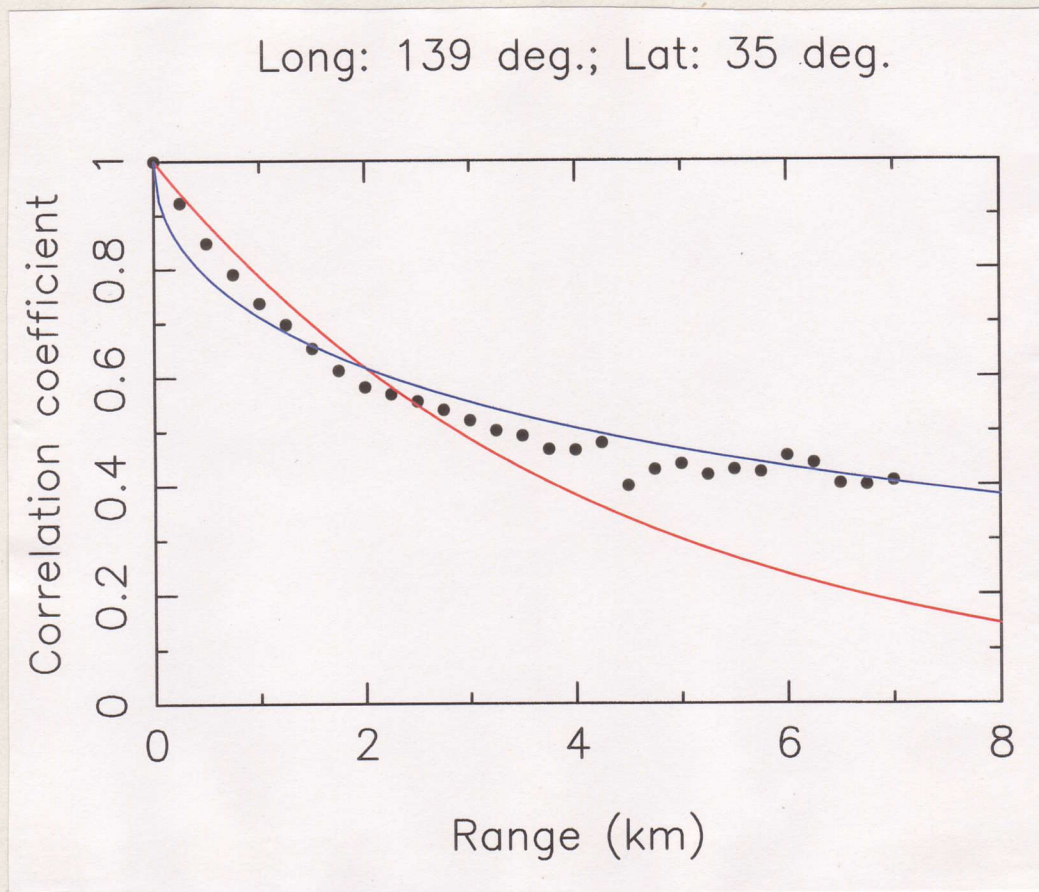


Fig. 3. An example of the spatial correlation function. Black dots are inferred from TRMM measurements. Red and blue curves are lines fitted by Eqs. (1) and (2), respectively.

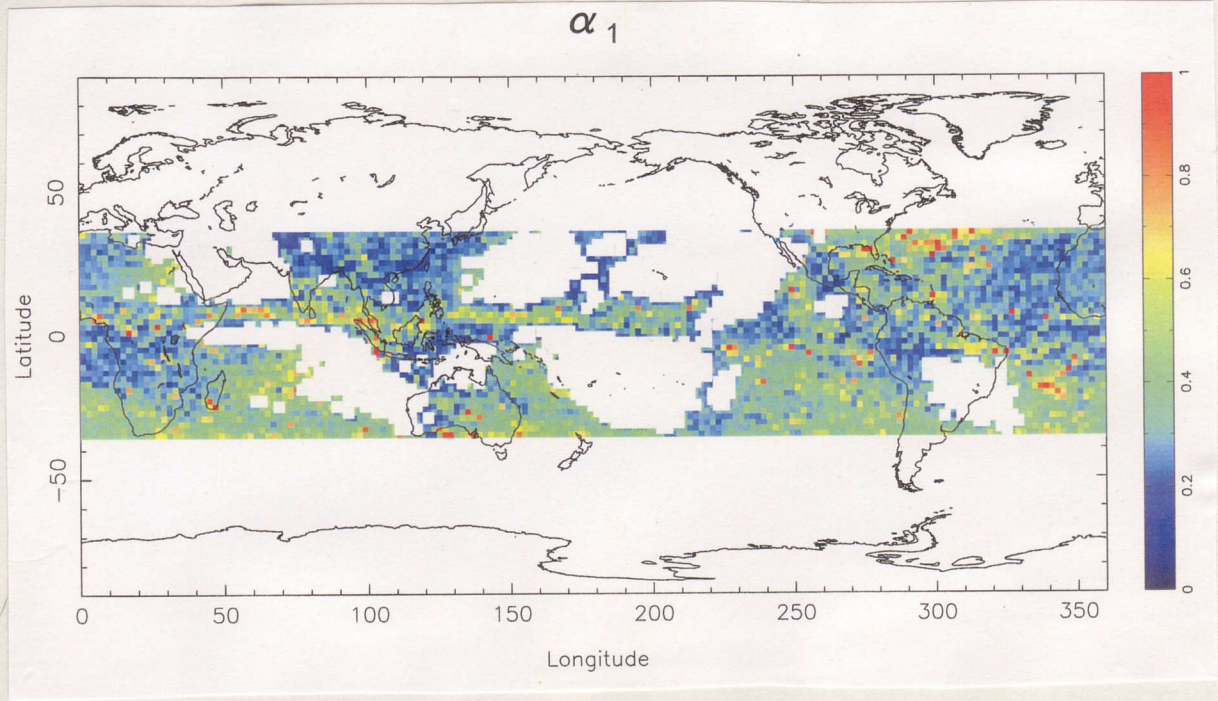


Fig. 4. Global distribution of α_1 . White gaps correspond to grids having large error of estimated parameter (larger than 100% of relative error). Color bar values indicate of α_1 .

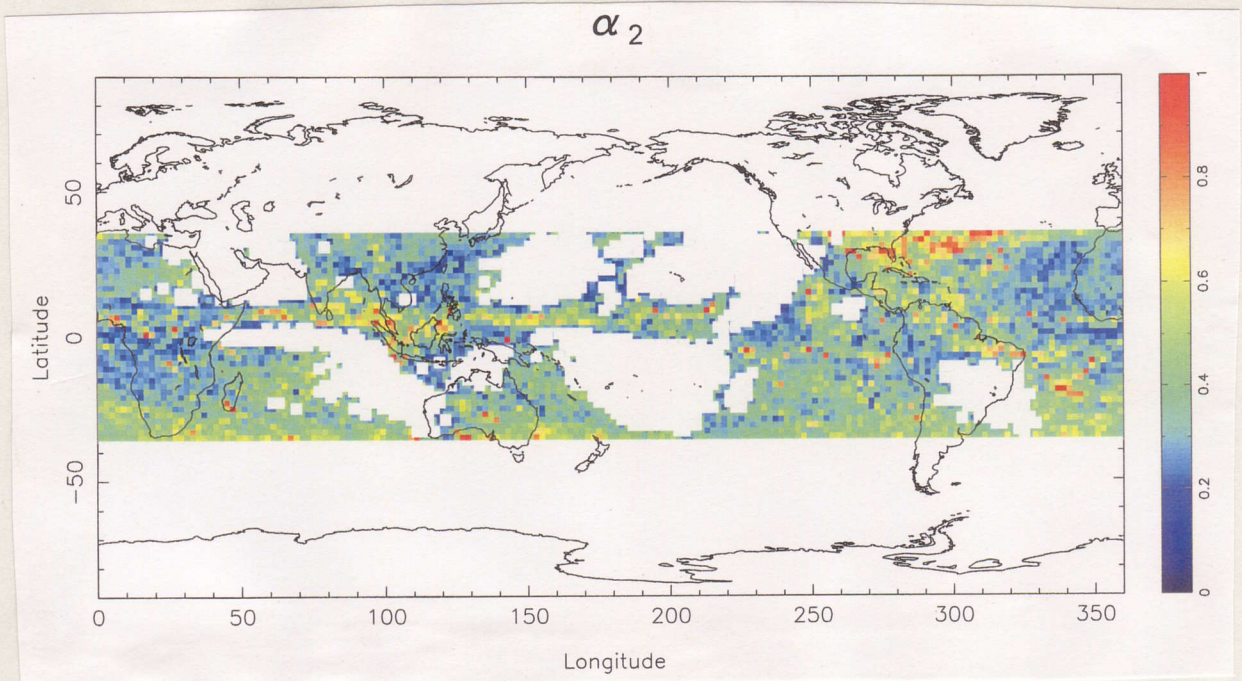


Fig. 5. Global distribution of α_2 . White gaps correspond to grids having large error of estimated parameter (larger than 100% of relative error). Color bar values indicate of α_2 .

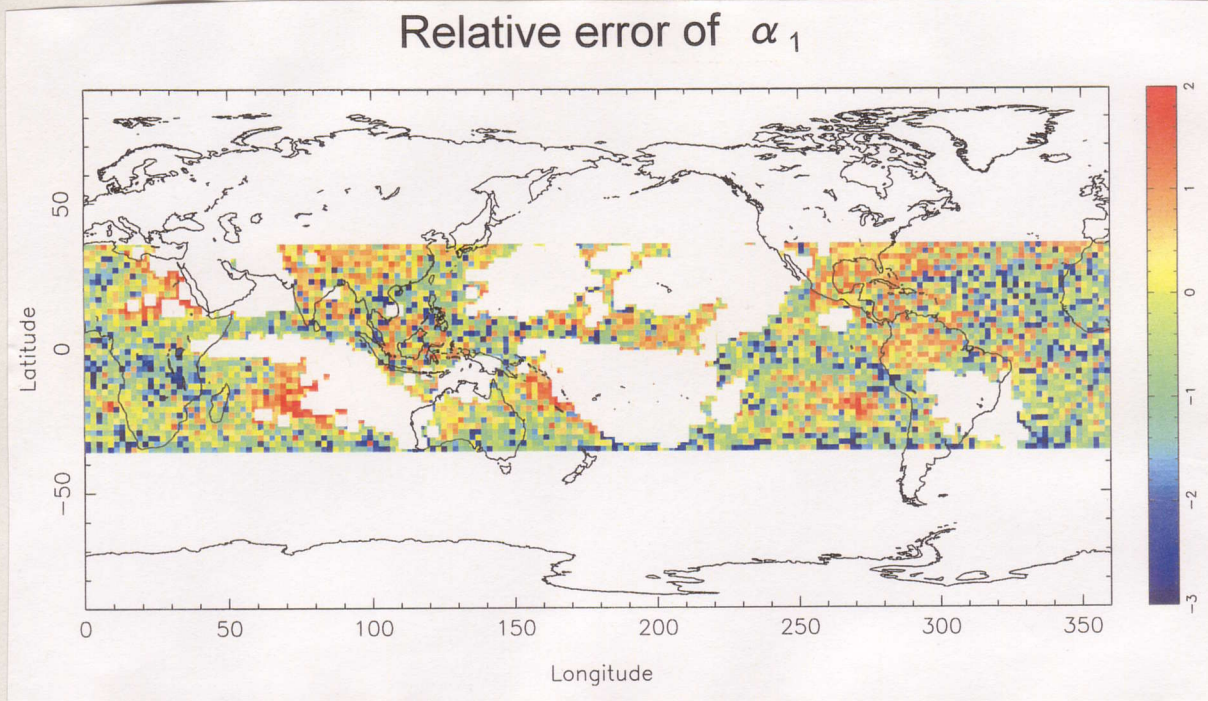


Fig. 6. Global distribution of relative error of α_1 . White gaps correspond to grids having large error of estimated parameter (larger than 100% of relative error). Color bar values indicate logarithms of relative error.

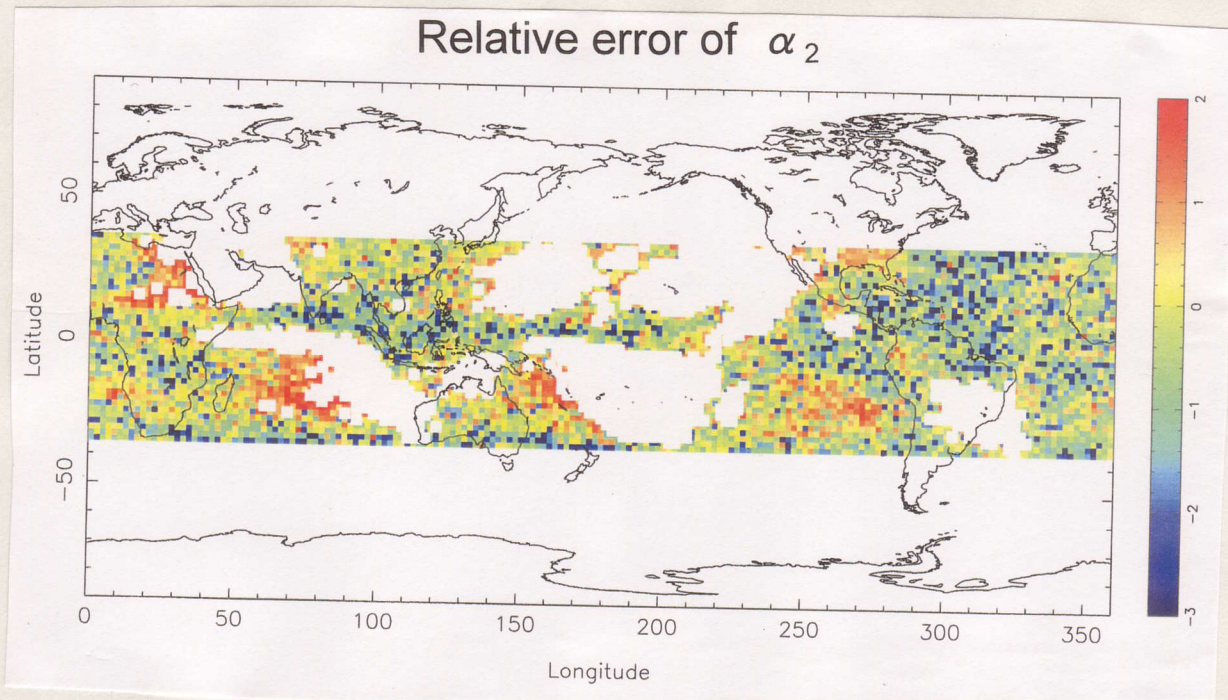


Fig. 7. Global distribution of relative error of α_2 . White gaps correspond to grids having large error of estimated parameter (larger than 100% of relative error). Color bar values indicate logarithms of relative error.